SMOOTH SURFACE RECONSTRUCTION FROM SPARSE DATA: COMPARISON OF SVSF AND 3DHM ALGORITHMS

Ahmad Almhdie[1], Christophe Léger[1] and Maïtine Bergounioux[2]
[1] LESI, Polytech'Orléans, Université d'Orléans, Orléans, France
[2] MAPMO, Faculté des Sciences, Université d'Orléans
E-mails: {ahmad.almhdie, christophe.leger}@univ-orleans.fr and Maitine.Bergounioux@labomath.univ-orleans.fr

ABSTRACT

We present in this paper an algorithm for surface reconstruction using thin plate splines on scattered patches or points on smooth surfaces. The algorithm is an improved version of Szeliski's Variational Spline Fitting algorithm (SVSF). In particular, we introduce a different derivation of the discrete equations for the energy corresponding to the thin plat model. The results obtained on simulated data show that our proposed algorithm converges faster than the original algorithm. To complete this study, we also discuss the choice of the algorithm's parameters in details using a cross validation technique. Finally, we compare our results to those obtained using a 3D Harmonic modelling (3DHM) Fourier-based algorithm (previously developed by the authors). We show that the proposed algorithm gives the best performance under a small sample size condition. However, when considering surfaces with a small percentage of the missing points, the 3DHM algorithm outperforms the other two spline-based algorithms.

1. INTRODUCTION

Surface reconstruction and smoothing methods are widely used in practice to best estimate the original surface represented by a scattered noisy point set arising in a number of medical imaging applications [1,2]. For instance, the number and the distribution of the initial samples of an organ surface lead to incomplete meshes. The problem of surface reconstruction can be solved using a variety of techniques: triangulation methods such as a Delaunay triangulation [3], deformable models [4] such as thin plate model [5], and Fourier-based interpolation methods [6], to mention a few. The former two approaches were selected for further study in this work as these are generally more appropriate for smooth surfaces such as left ventricle surfaces.

1.1. The Thin Plate Model

In [7], Szeliski proposed to use a deformable model to estimate the missing points (here we call it SVSF). In his algorithm, the problem is formulated as an optimization one. The function to be minimized is written:

$$E(x) = E_d(x) + \lambda E_s(x) \qquad (1)$$

where $x_{i,j}$ ($i = 0{:}N\text{-}1$, $j = 0{:}M\text{-}1$) are the mesh regular points. This function includes two constraints: the data compatibility constraint $E_d(x)$, and the smoothness constraint $E_s(x)$. The regularization parameter λ ($\lambda>0$) is used to adjust the closeness of the fit between the surface and the sparse data set. This parameter depends on the sparse data set and can be estimated using a generalised cross validation technique.

The above formulation is usually expressed as an energy minimisation problem where an attracting force draws the mesh towards the sparse data and a tension in the mesh keeps the surface smooth [8]. For very high values of λ, $(\lambda \approx \infty)$, the fitted surface tends towards a flat one.

The data compatibility constraint measures the distance between the original sparse points and the interpolated smooth surface. The expression for the discrete energy corresponding to the function above can also be written as [7]:

$$E_d(x,d) = \frac{1}{2}\sum_{(i,j)} w_{i,j}(x_{i,j} - d_{i,j})^2 \qquad (2)$$

where $d_{i,j}$ ($d_{i,j} = 0$ at missing points) are the points of the original sparse surface and the weights $w_{i,j}$ ($w_{i,j} = d_{i,j}$) are inversely related to the variance of the measurements.

Using the thin plate model [7], the smoothness constraint can be written as:

$$\varepsilon_s(f) = \frac{1}{2}\int\int\left(f_{uu}^2 + 2f_{uv}^2 + f_{vv}^2\right)dudv \qquad (3)$$

2. IMPROVED ALGORITHM

In this work, we propose a more accurate derivation process to get the discrete energy corresponding to the above function. In particular, we propose to use the following approximation E_p for ε_s :

$$E_p(x) = \frac{h_x h_y}{2} \sum_{i,j} \left[\left(\frac{x_{i+1,j} - 2x_{i,j} + x_{i-1,j}}{h_x^2} \right)^2 + \left(\frac{x_{i,j+1} - 2x_{i,j} + x_{i,j-1}}{h_y^2} \right)^2 + \frac{1}{8} \left(\frac{x_{i+1,j+1} - x_{i+1,j-1} - x_{i-1,j+1} + x_{i-1,j-1}}{h_x h_y} \right)^2 \right] \quad (4)$$

where $h_x = |\Delta x|$ and $h_y = |\Delta y|$ are the step sizes of the mesh in the x and y directions respectively. The approximation above is more accurate as it uses the so called 5-star points scheme (that is positions: $(i-1, j-1), (i-1, j+1), (i+1, j-1), (i+1, j+1)$, to approximate the second-order derivative at position (i, j) while Szeliski's approach only uses the biased forward positions $(i, j), (i, j+1), (i+1, j), (i+1, j+1)$, (see [7] for details).

The above approximation was found to lead to faster convergence of the iterative conjugate gradient method (used for finding the solution of the overall discrete energy function of equation (7)), compared to Szeliski's original approximation.

Reassembling all mesh points into a vector $\mathbf{x}$, one can rewrite equations (2) and (4) in a matrix form. The energy corresponding to the data compatibility constraint becomes:

$$E_d(\mathbf{x}, \mathbf{d}) = \frac{1}{2}(\mathbf{x} - \mathbf{d})^T \mathbf{A}_d (\mathbf{x} - \mathbf{d}) \quad (5)$$

where d is a zero-padded vector of data values and the diagonal matrix $\mathbf{A}_d$ has entries w_i at which the data coincide with the sparse data points and zeros elsewhere. In particular, this allows to treat problems with missing or unknown data.

The energy corresponding to the thin plate model can also be written in compact form as:

$$E\ (\mathbf{x}) = \frac{1}{2} \mathbf{x}^T \mathbf{A}_s \mathbf{x} \quad (6)$$

where the *stiffness* matrix $\mathbf{A}_s$ is a sparse matrix block diagonal matrix. It has at most 13 entries per row [7]. The combined discrete energy expression can hence be written in matrix form as:

$$E(\mathbf{x}) = \frac{1}{2} \mathbf{x}^T \mathbf{A}\, \mathbf{x} - \mathbf{x}^T \mathbf{b} + c \quad (7)$$

Where $\mathbf{A} = \lambda \cdot \mathbf{A}_s + \mathbf{A}_d, \mathbf{b} = \mathbf{A}_d \cdot \mathbf{d}$ and c is a constant that may be omitted in the minimization process.

This energy function has a minimum at $\mathbf{x} = \mathbf{x}^*$, which is the solution of the following linear system:

$$\mathbf{A}\, \mathbf{x}^* = \mathbf{b} \quad (8)$$

since A is a strictly positive matrix. The above set of linear equations is, hence, a high dimension homogeneous positive definite system, that can be solved using the conjugate gradient method, thanks to the strict positivity of the matrix A.

3. 3DHM FOURIER-BASED ALGORITHM

For comparison purposes, we considered the use of the 3DHM [3D Harmonic Modelling] algorithm (developed previously by the authors). This algorithm is much less complex than the previous thin plate splines algorithm. The 3DHM algorithm reconstructs the incomplete surface using an iterative algorithm based on Fourier analysis. This algorithm consists of four major steps (per iteration):

A. The 2D Fourier transform $D(u, v)$ of the k^{th} doubly periodic mesh $x_{i,j}^k$ is computed:

$$D(u, v) = \Im\left[x_{i,j}^k\right] \quad (9)$$

B. The resulting $D(u, v)$ is low-pass filtered to reduce discontinuities in the space domain. The transfer function of such filter is given by:

$$H(u, v) = \begin{cases} 1 & \text{if } |u| < U_0 \text{ and } |v| < V_0 \\ 0 & \text{if not} \end{cases} \quad (10)$$

C. The missing points are then estimated using the inverse Fourier transform:

$$x_{i,j}^{k+1} = \Im^{-1}[H(u, v).D(u, v)] \quad (11)$$

D. Termination criterion: Terminate the iterations when the Mean Square Error between the estimated values of the missing points from successive iterations falls below a preset threshold ζ. If not, the algorithm restarts using the recently generated mesh $(k = k + 1)$ as an input to step A (the data from the initial sparse mesh is retained).

The mean square error (MSE) between successive surfaces is written:

$$\frac{1}{N.M}\sum_{i=0}^{N}\sum_{j=0}^{M}\left[x_{i,j}^{k}-x_{i,j}^{k+1}\right]^{2} \qquad (12)$$

4. SIMULATION RESULTS AND DISCUSSION

Our first aim was to compare the convergence characteristics of the original and modified Szeliski algorithm for relatively smooth surfaces. We then compared the performance of the modified algorithm and that of the 3DHM algorithm. In order to limit the scope of the problem, we adopted the following methodology for choosing the optimal values for the control parameters (λ, w):

A. Choose a smooth surface as a reference model.
B. Randomly select about 10% of the total surface patches.
C. Reconstruct the surface using these selected patches.
D. Calculate the mean square error between the reconstructed surface and the reference model using different values of (λ, w).

Figure 1 presents a reference model of 32×32 smooth mesh, and Figure 2 shows a mesh of the randomly selected 92 patches. Using the proposed algorithm, Figure 3 shows the reconstructed surface.

Figure 4 displays the MSE as a function of (λ, w). Notice that the MSE almost stabilizes when w is greater than 300 and λ is less than 30. w =314 is actually the inverse of the variance of the selected patches [7].

The results displayed in Figure 5 show clearly that the proposed algorithm, SVSF, outperforms the original SVSF algorithm, e.g., when the tolerance value of the iterative conjugate gradient algorithm is set to 10^{-4}, the modified algorithm converges about 100 iterations faster than the original algorithm. One can also notice that the inappropriate choice of w and λ can lead to substantial deterioration in performance.

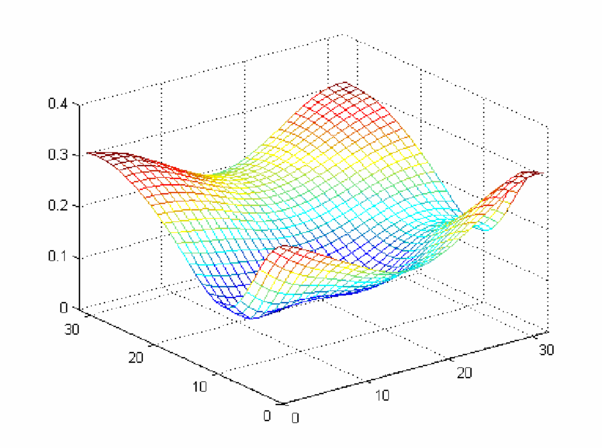

Figure 1. Typical 32×32 smooth surface.

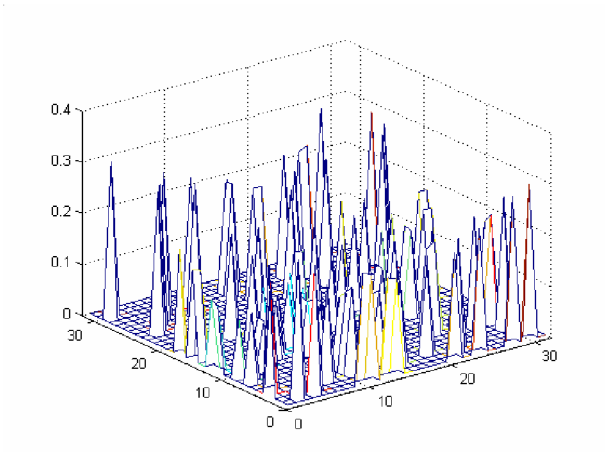

Figure 2. Randomly selected 92 patches from the surface in Figure 1.

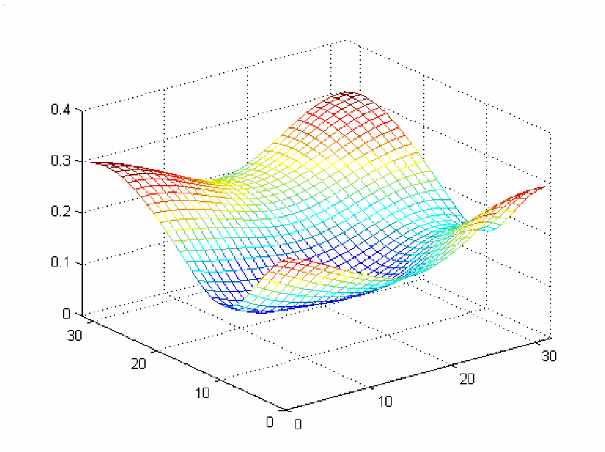

Figure 3. Reconstructed surface using the proposed algorithm.

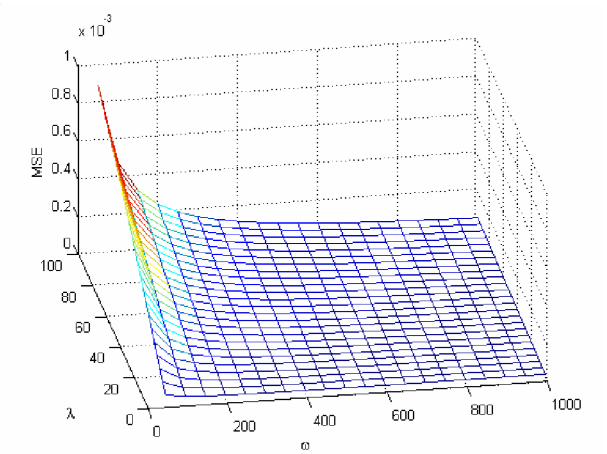

Figure 4. The MSE vs w and λ.

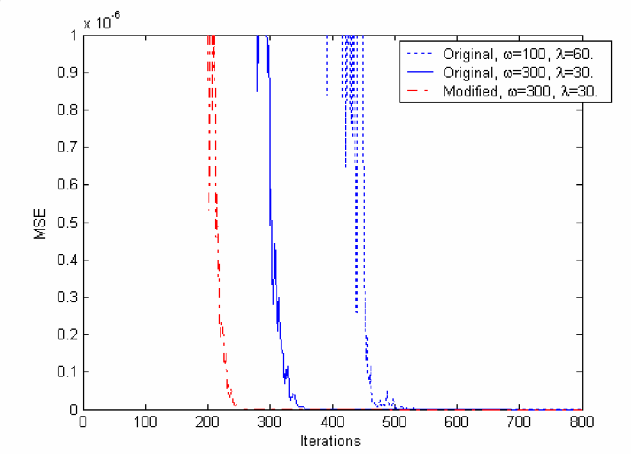

Figure 5. Rate of convergence of the conjugate gradient algorithm.

To complete the performance analysis of the proposed algorithm, we considered three different scenarios: small, medium, and large sample sizes. A set of 32, 92, 768 sparse patches were respectively chosen (randomly selected points).

As expected, with a very small number of sparse patches, both the modified and the original Szeliski algorithms performed better than the 3DHM algorithm. As can be seen from Figure 6, the 3DHM can not achieve an MSE of the ratio of 10^{-4}, while both other algorithms achieved such tolerance in less than 300 iterations.

However, as the number of missing patches gets lower, the 3DHM algorithm outperforms both the original and modified Szeliski algorithms, as can been seen from Figure 8 which corresponds to the third scenario. In Figure 7, which corresponds to the second scenario, where about only 10% of the total mesh patches were chosen, the 3DHM also performs better than the other two algorithms. However, it takes more iterations to converge if we take the computation time into consideration as shown in Table 1. For example, doing 300 iterations takes about 10 seconds for the original and modified algorithm, whereas it takes less than 0.5 second for the 3DHM algorithm.

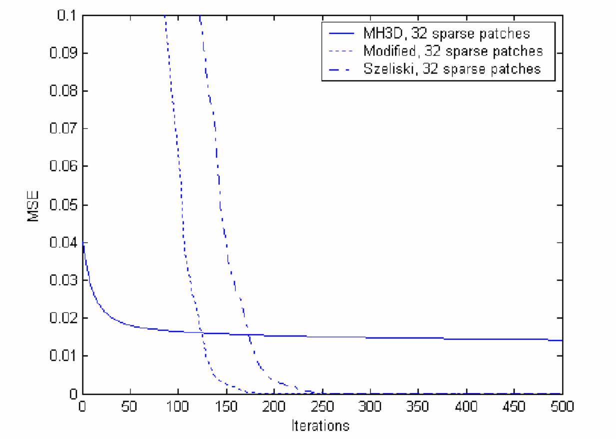

Figure 6. MSE comparison for the 1st scenario.

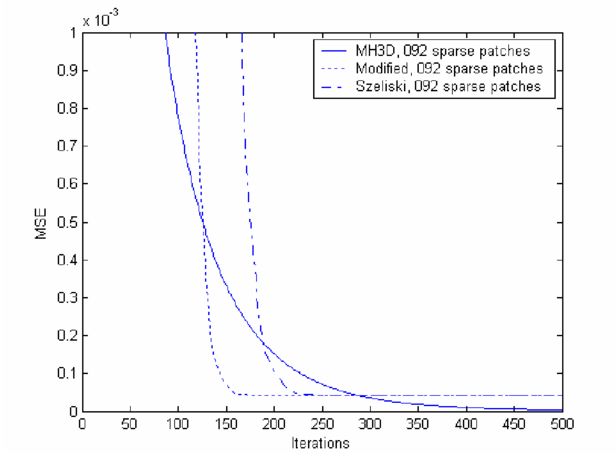

Figure 7. MSE comparison for the 2nd scenario.

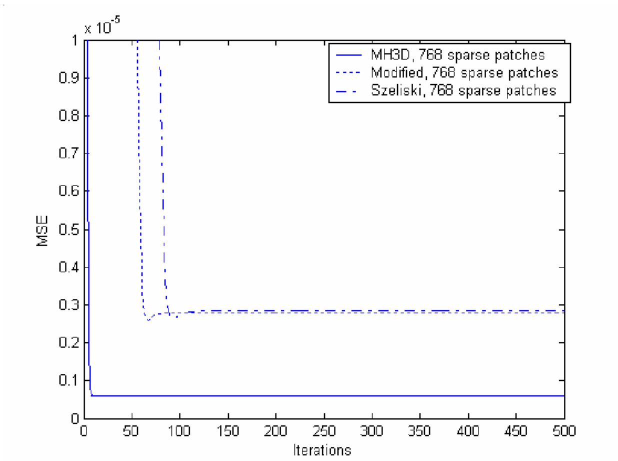

Figure 8. MSE comparison for the 3rd scenario.

	Modified Szeliski		Original Szeliski		3DHM	
	K	τ (seconds)	K	τ (seconds)	K	τ (seconds)
1st scenario	208	7.07	285	9.89	Very large	-
2nd scenario	144	4.96	202	6.82	228	0.38
3rd scenario	50	1.79	70	2.49	3	0.02

Table 1. Number of iterations (K) and their corresponding computation times (τ) for the different sample sizes.

5. CONCLUSION

In this paper, we presented an improved implementation of the Variational Spline Fitting Algorithm. The algorithm is based on a more general and precise approximation of the energy equations in discrete time. We have shown that the modified algorithm outperforms the original implementation discussed by Szeleski. When compared to the 3DHM Fourier based algorithm developed earlier by the authors, the proposed algorithm is found to best suit the case of size sample. This proposed algorithm is easy to implement and converges faster than the original one. Moreover, we have shown that the proposed algorithm can be extremely useful when the observations sample size is very small. However, as the percentage of the missing points decreases, the performance of the MH3D algorithm performs the best. We are currently investigating the potential of such algorithm in practical medical applications of surface reconstruction where very limited data is available.

6. REFERENCES

[1] García O., Susín A. ‘*Left Ventricle's Surface Reconstruction and Volume Estimation*’. 3es. Jornades de Recerca en Enginyeria Biomèdica. Lacroix D., Ginebra M.P. ed pp.1-10 (2002) Xarxa Temàtica en Enginyeria Biomèdica (ISBN 84-699-8705-4). Vic (Spain).

[2] Jonathan C. Carr, ‘*Surface Reconstruction in 3D Medical Imaging*’, Thesis, Dept. Electrical and Electronic Engineering, University of Canterbury, Christchurch, New Zealand, February 1996.

[3] S. Gao, H.-Q. Lu, ‘*A Fast Algorithm for Delaunay Based Surface Reconstruction*’, the 11th International Conference in Central Europe on Computer Graphics, Visualization and Computer Vision (WSCG 2003).

[4] Y.F. Wang, J. F. Wang, ‘*Surface Reconstruction Using Deformable Models with Interior and Boundary Constraints’*, IEEE Transactions on Pattern Analysis and Machine Intelligence, vol. 14, no.5, pp. 572-579, May 1992.

[5] R. Enciso, John P. Lewis, U. Neumann, and J. Mah, *’3D Tooth Shape from Radiographs using Thin-Plate Splines’*, The 11th Annual Medicine Meets Virtual Reality Conference, Newport Beach, California, January 2003, pp. 22-25.

[6] Cl. Bonciu, R. Weber, C. Léger, ‘*4D reconstruction of the left ventricle during a single heart beat, from ultrasound imaging*’, Image and Vision Computing, Elsevier Eds, vol. 19, no. 6, pp 401-412, April 2001.

[7] Richard SZELISKI, *‘Fast Surface Using Hierarchical Basis Function’*, IEEE Transaction on Pattern analysis and machine intelligence, vol. 12, no. 6, pp. 513-528, June 1990.

[8] H. Hope, T. DeRose, T. Duchamp, M. Halstead, J. Hin, H. McDonald, J. Schweitzer, and W. Stuetzle, ‘*Surface reconstruction from Unorganized Points,*’ Computer Graphics Proceedings, vol. 26, pp 71-77, July 1992.